Early Detection of Preterm Intraventricular Hemorrhage From Clinical Electroencephalography

Kartik K. Iyer, PhD[1,2]; James A. Roberts, PhD[1]; Lena Hellström-Westas, MD, PhD[3]; Sverre Wikström, MD, PhD[4]; Ingrid Hansen Pupp, MD, PhD[5]; David Ley, MD, PhD[5]; Michael Breakspear, MBBS, PhD[1,6]; Sampsa Vanhatalo, MD, PhD[7,8]

Objectives: Intraventricular hemorrhage is a common neurologic complication of extremely preterm birth and leads to lifelong neurodevelopmental disabilities. Early bedside detection of intraventricular hemorrhage is crucial to enabling timely interventions. We sought to detect early markers of brain activity that preempt the occurrence of intraventricular hemorrhage in extremely preterm infants during the first postnatal days.

Design: Cross-sectional study.

Setting: Level III neonatal ICU.

Patients: Twenty-five extremely preterm infants (22–28 wk gestational age).

Measurements and Main Results: We quantitatively assessed electroencephalography in the first 72 hours of postnatal life, focusing on the electrical burst activity of the preterm. Cranial ultrasound was performed on day 1 (0–24 hr) and day 3 (48–72 hr). Outcomes were categorized into three classes: 1) no intraventricular hemorrhage (grade 0); 2) mild-moderate intraventricular hemorrhage (grades 1–2, i.e., germinal matrix hemorrhages or intraventricular hemorrhage without ventricular dilatation, respectively); and 3) severe intraventricular hemorrhage (grades 3–4, i.e., intraventricular hemorrhage with ventricular dilatation or intraparenchymal involvement). Quantitative assessment of electroencephalography burst shapes was used to preempt the occurrence and severity of intraventricular hemorrhage as detected by ultrasound. The shapes of electroencephalography bursts found in the intraventricular hemorrhage infants were significantly sharper ($F = 13.78$; $p < 0.0001$) and less symmetric ($F = 6.91$; $p < 0.015$) than in preterm infants without intraventricular hemorrhage. Diagnostic discrimination of intraventricular hemorrhage infants using measures of burst symmetry and sharpness yielded high true-positive rates (82% and 88%, respectively) and low false-positive rates (19% and 8%). Conventional electroencephalography measures of interburst intervals and burst counts were not significantly associated with intraventricular hemorrhage.

Conclusions: Detection of intraventricular hemorrhage during the first postnatal days is possible from bedside measures of brain activity prior to ultrasound confirmation of intraventricular hemorrhage. Significantly, our novel automated assessment of electroencephalography preempts the occurrence of intraventricular hemorrhage in the extremely preterm. Early bedside detection of intraventricular hemorrhage holds promise for advancing individual care, targeted therapeutic trials, and understanding mechanisms of brain injury in neonates. (*Crit Care Med* 2015; 43:2219–2227)

Key Words: cortical burst shape; electroencephalography; intraventricular hemorrhage; neonatal intensive care; preterm; ultrasound

[1]Systems Neuroscience Group, QIMR Berghofer Medical Research Institute, Brisbane, QLD, Australia.

[2]School of Medicine, Faculty of Medicine and Biomedical Sciences, University of Queensland, QLD, Australia.

[3]Department of Women's and Children's Health, Uppsala University, Uppsala, Sweden.

[4]Department of Pediatrics, Karlstad Central Hospital, Karlstad, Sweden.

[5]Department of Pediatrics, Institute for Clinical Sciences, Lund University, Lund, Sweden.

[6]Metro North Mental Health Service, Brisbane, QLD, Australia.

[7]Department of Children's Clinical Neurophysiology, HUS Medical Imaging Center, Helsinki University Central Hospital and University of Helsinki, Helsinki, Finland.

[8]Department of Pediatrics, Children's Hospital, University Central Hospital and University of Helsinki, Helsinki, Finland.

Dr. Hellström-Westas is employed by Uppsala Universitet, provided expert testimony for the Swedish National Board of Health and Welfare, received royalties from Informa Healthcare (co-author of An Atlas of Amplitude Integrated EEGs in the Newborn), and received support for article research from the Swedish Research Council and the Linnea and Josef Carlsson Foundation. Her institution received grant support from the Swedish Research Council and the Linnea and Josef Carlsson Foundation. Dr. Breakspear received support for article research from the National Health and Medical Research Council (Australia: grants 1037196 and 510135). Dr. Vanhatalo was supported by the Academy of Finland grant 253130 and Juselius Foundation. The remaining authors have disclosed that they do not have any potential conflicts of interest.

For information regarding this article, E-mail: kartik.iyer@uqconnect.edu.au

DOI: 10.1097/CCM.0000000000001190

Preterm infants are at an increased risk of acute neurologic disorders, such as germinal matrix and intraventricular hemorrhage (IVH), during the first few days of life (1, 2). Common pathophysiologic mechanisms that lead to

IVH include failure of cerebral autoregulation (3, 4), hypoxic-ischemic insults, and sepsis (5). Prevention and management of IVH focuses on systemic circulatory stabilization and cardiorespiratory support as well as correction of coagulopathies (1, 6). An acute injury such as a large IVH predisposes an infant to poor neurodevelopmental outcomes (2) such as cerebral palsy, developmental delay, or hydrocephalus (7). Hence, prevention or early detection of IVH holds promise for significantly improving neurodevelopmental outcomes in these vulnerable neonates.

The current gold standard for IVH detection is cranial ultrasonography through the anterior fontanel which is sensitive to lesions within hours to days after the occurrence of IVH (6, 8). A timely therapeutic response to IVH requires a means of preempting IVH or detecting it as soon as it occurs, implying a need for continuous brain monitoring. Studies have shown that IVH may cause a qualitative change in electroencephalography (EEG) waveforms—as visually assessed (9)—or in the EEG background activity (10–12). Continuous EEG recording is hence recognized as a clinically useful method for monitoring the preterm brain and is in widespread use (13–15). Identification of EEG features appropriate for automatic and objective analysis would greatly enhance the potential for EEG monitoring to be used for real-time detection of impending IVH.

The hallmark of early EEG activity in extremely preterm infants is the presence of intermittently occurring bursts, or spontaneous activity transients (SATs), evident in the EEG trace as irregular high-amplitude bursts of activity (16, 17). Normal preterm EEG activity is characterized by intermittent occurrence of activity with mixed frequency content and the relatively silent EEG during the interburst interval (IBI) periods (17). In particular, extremely early preterm infants (< 28 wk gestational age) have characteristically dominant few second long epochs of low-frequency activity (< 1 Hz) with superimposed fast activity periods, collectively called "bursts," SATs, or delta brushes (16, 18). Abnormalities in the preterm EEG are mostly seen in durations of the silent periods (17); however, visually observed changes in the waveforms, such as positive rolandic sharp (PRS) waves, have also been reported (19).

We recently developed a quantitative method to rapidly analyze the EEG bursts that occur during burst-suppression EEG after asphyxia in full-term infants (20) and found that specific changes in burst size are predictive of long-term outcome (21). These methods are fully automated and free from subjective qualitative assessments, thus enabling robust burst characterization and complementing conventional visually analyzed EEG measures such as the IBI and burst counts (21, 22). In the present study, we hypothesized that quantitative measures of the early cortical bursts in the preterm EEG may acutely reflect, and even precede, the onset of IVH during the first days of life. Importantly, our findings suggest that IVH may be detectable via bedside EEG monitoring prior to routine cranial ultrasound detection, hence our method opens a novel window to real-time monitoring as well as identifying neural mechanisms underlying IVH.

MATERIALS AND METHODS

Data Collection and Analysis

We analyzed EEG recordings of 25 preterm infants (gestational age, 22–28 wk; **Table 1**) that were monitored during their first 3 days of life in the neonatal ICU (NICU) at Lund University Hospital, Sweden. The infants were part of a larger prospectively recruited cohort of extremely preterm infants from which qualitative and quantitative (IBI and measures of suppression) EEG analyses have been previously published (15, 22, 23). Inclusion criteria were age less than 28 weeks of gestation, availability of artifact-free EEG epochs at postnatal hours 12–72, as well as clinically confirmed absence or presence of IVH via ultrasound at either day 1 or day 3 of life. EEG was acquired at the biparietal P3-P4 derivation at a sampling rate of 256 Hz using a NicOne amplifier (Cardinal Healthcare, Nicolet Biomedical, Madison, WI). Epochs of EEG (90–120 min) were selected at fixed postnatal time points of 12, 24, 48, and 72 hours irrespective of vigilance state. Our quantitative EEG analysis focused on EEG epochs that preceded or followed the confirmation of hemorrhage by ultrasound within the first 3 days of birth. The use of patient data for this study was approved by the Research Ethics Committee at Lund University.

Cranial ultrasound was performed routinely on day 1 (0–24 postnatal hours) and day 3 (48–72 postnatal hours) (Acuson XP 512, 7.5 MHz transducer, or Acuson Sequoia 8.5 MHz, Mountain View, CA). Data were analyzed in three categories according to the severity of IVH: no IVH (grade 0); mild-moderate IVH (grades 1–2, i.e., germinal matrix hemorrhages or IVH without ventricular dilatation, respectively); and severe and very severe IVH (grades 3–4, i.e., IVH with ventricular dilatation or intraparenchymal involvement, respectively) (24). Clinical details for each neonate are provided in Table 1.

Contrasts on EEG analyses were then performed, comparing: 1) infants with no IVH, 2) infants with IVH grades 1–2 (mild-moderate), and 3) IVH grades 3–4 (severe IVH). We also analyzed bursts from EEG epochs recorded prior to identification of the IVH by ultrasound to investigate whether burst shapes could indicate an impending or early-onset phase of IVH. Thus, we compared all postnatal epochs with ultrasound-confirmed IVH with epochs temporally precedent to hemorrhage confirmation. Hereafter, we refer to epochs with no hemorrhage as "no IVH"; epochs prior to ultrasound-confirmed IVH as "pre-US-IVH"; and epochs with ultrasound-confirmed IVH as "US-IVH." Eleven neonates were identified as no IVH epochs. For mild-moderate IVH, 12 epochs were identified as pre-US-IVH grade 1–2 and 11 epochs as US-IVH grade 1–2. For severe IVH, six epochs were identified as pre-US-IVH grade 3–4 and four epochs as US-IVH grade 3–4.EEG data were exported to MATLAB (Mathworks, Natick, MA), band-pass filtered (0.2–20 Hz), and analyzed using conventional and custom algorithms (18). We first applied conventional analyses, namely IBI and burst counts, for the three preterm populations as classified in Table 1. We then used custom algorithms to calculate changes in burst symmetry (skewness, Σ) and sharpness (kurtosis, K), across a wide range of burst durations (200 ms to 6 s) (cf. [18]).

TABLE 1. Clinical Summary of the Preterm Population Analyzed for This Study

Subjects	Gestational Age (Wk + D)	Birth Weight (g)	Apgar Score at 5 Min[a]	US Day 1 (0–24 Hr)	US Day 2 (24–48 Hr)	US Day 3 (48–72 Hr)
No IVH						
1	26+6	854	6	0		0
2	25+2	638	7	0		0
3	27+1	854	8	0		0
4	24+4	788	8	0		0
5	27+3	840	7	0		0
6	25+3	940	8	0		0
7	27+3	950	9	0		0
8	27+3	1148	8	0		0
9	25+1	732	9	0		0
10	25+5	946	5	0		0
11	25+5	780	8	0		0
IVH (grade 1–2)						
12	24+2	730	6	0		1
13	24+2	646	5	2		2
14	26+4	951	8	1		1
15	25	725	6	0		2
16	27	970	7	1		2
17	23+5	584	9	0		2
18	27+4	1092	6	–	2	2
19	28+1	1230	7	–	2	2
20	27+4	630	6	–	2	2
IVH (grade 3–4)						
21	22+6	580	7	0		3
22[b]	26+4	670	3	4		–
23[c]	24+3	796	6	0		3
24[c]	27	950	7	0	3	–
25	24+2	730	6	3		–

US = cranial ultrasound, IVH = intraventricular hemorrhage.

[a]IVH and Apgar score at 5 min were significantly correlated (Wilcoxon rank-sum test, $p < 0.05$).

[b]Periventricular leukomalacia (25).

[c]Bilateral IVH.

Ultrasound labels: 0 = no IVH, 1 = mild IVH, 2 = moderate IVH, 3 = severe IVH, 4 = very severe IVH, "–" = no ultrasound examination, and blank table entry = no ultrasound performed.

Statistical group comparisons of burst shape metrics were conducted using one-way analysis of variance. **Figure 1** shows a schematic for the analyses.

To assess diagnostic accuracy of burst shapes to identify IVH, we estimated true-positive and false-positive rates across a range of Σ and *K* values, deriving corresponding receiver operating characteristic (ROC) curves. The ROC curves were further quantified by calculating the area under the curve (AUC), a measure of diagnostic accuracy. We then summarized the clinical sensitivity and specificity of burst symmetry and sharpness values to discriminate between pre-US-IVH, US-IVH, and no IVH neonates. To validate the diagnostic accuracy of our measures, we performed two tests of data reliability for both Σ and *K* values. First, we used the leave-one-out cross-validation test—a method where one single value in the sample set is tested against the rest of the samples. This process is iteratively repeated for each value to calculate the error in prediction, until all samples in the dataset have been tested,

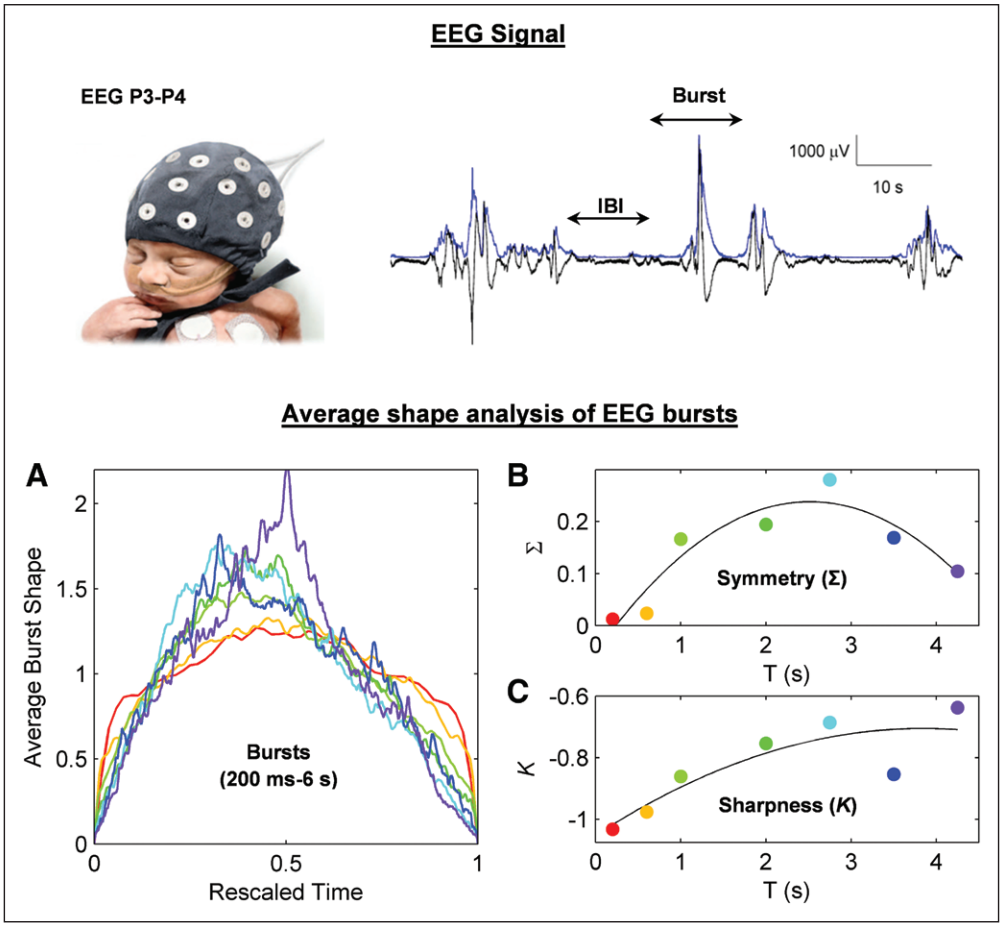

Figure 1. Analysis schematic for each electroencephalography (EEG) burst. The biparietal P3-P4 signal is filtered before extracting bursts using an adaptive threshold technique on the signal envelope (*blue overlay* in EEG trace). **A**, Bursts are binned into seven groups according to duration (*T*). Average shapes are calculated for each group and rescaled to have unit duration and area. Average shapes are analyzed for their change in shape symmetry (skewness) (**B**), and sharpness (kurtosis) (**C**) as a function of duration *T*. Durations in average burst shapes are here color coded to corresponding points in the symmetry and sharpness graphs: 200 ms (*red*), 600 ms (*yellow*), 1 s (*light green*), 2 s (*green*), 2.75 s (*cyan*), 3.5 s (*blue*), and greater than 4.25 s (*purple*). *Solid lines* show quadratic fits to symmetry and sharpness graphs across burst durations. IBI = interburst interval.

thus deriving an overall accuracy measure. Comparatively, we used the leave-one-out method to perform another test of accuracy by adding null data points in each sample set—group mean values of Σ and *K* in both no IVH and IVH infants, respectively—and derived the relevant sensitivity and specificity measures.

RESULTS

Conventional Analyses

Conventional EEG measures did not differ significantly between the groups. In particular, counts of IBIs with length greater than 1 second were comparable in the infants with and without IVH ($F = 0.08$; $p = 0.92$). Further, counts comparing the number of short bursts ($F = 0.43$; $p = 0.65$ for bursts < 2 s) with long bursts ($F = 0.12$; $p = 0.88$ for bursts > 2 s) did not significantly differ (**Fig. 2, *A* and *B***). There were also no statistically significant differences in IBI or burst counts related to severity of IVH, gestational age or birth weight, or 5-minute Apgar score.

Visual inspection of the preterm EEG showed characteristic bursts (SATs) (16, 17) in both groups and suggested higher amplitudes and greater burst areas for infants with IVH than infants without IVH (examples shown in **Fig. 2, *C* and *E***). These differences appeared more evident when we computed the instantaneous amplitude of the signals (see blue overlay traces in Fig. 2, *C* and E) and superimposed hundreds of bursts (**Fig. 2, *D* and *F***). However, statistical comparison of conventional mean amplitudes ($F = 0.54$; $p = 0.59$) and mean areas ($F = 2.21$; $p = 0.14$) for bursts (> 2 s duration) did not significantly differ between groups. In summary, these findings suggest that the conventional measures (burst counts, IBIs, and amplitude changes) may not be able to distinguish EEG events in infants with IVH compared with those without IVH.

Burst Shape Analyses

We next examined the change in average burst shape as a function of burst duration using measures of burst symmetry (Σ) and sharpness (*K*). Visual comparison of grand average burst shapes across burst durations shows clear differences between the three IVH groups (**Fig. 3**). For each IVH grouping, we calculated average burst shapes for no IVH, pre-US-IVH grades 1–2 and 3–4 compared with US-IVH grades 1–2 and 3–4, respectively (**Fig. 3*A–E***). Most notably, there was a strong increase in the sharpness of longer bursts (> 2 s duration) with increasing severity of IVH. The longer bursts in infants with severe IVH (grades 3–4) were also skewed to the left, with sharper onset and slower decay compared to the bursts in infants with no or mild-moderate IVH (grades 1–2).

Statistical comparison of burst shapes between the three groups—no IVH, mild-moderate IVH 1–2, and severe IVH 3–4—showed that bursts in the IVH infants were significantly sharper (higher *K*) at most burst durations (**Fig. 4*A***). Mean *K* values for bursts longer than 2 seconds differed markedly between no IVH and IVH infants (pre-US-IVH: $F = 22.23$, $p = 6.5 \times 10^{-5}$; US-IVH: $F = 22.25$, $p = 8.5 \times 10^{-5}$) (**Fig. 4*B***). We also observed that asymmetry (Σ) of

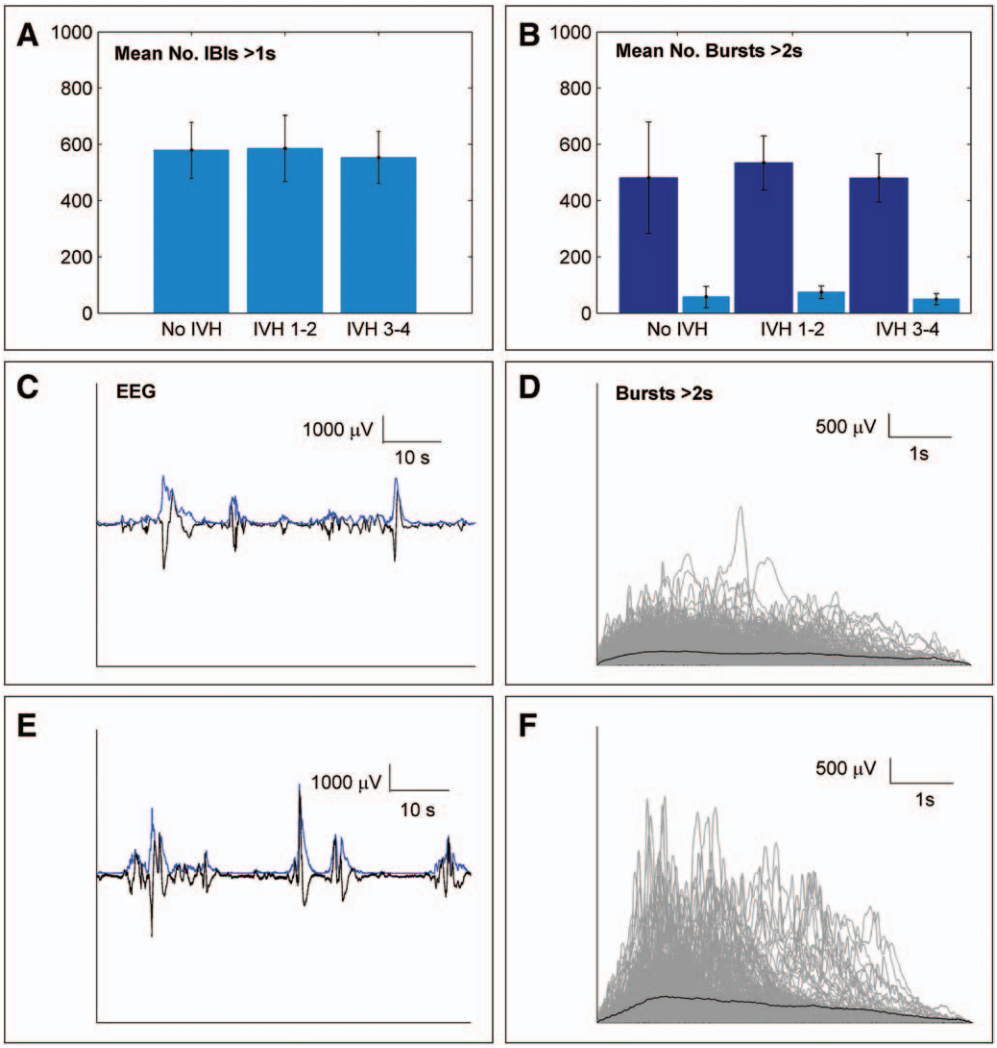

Figure 2. Conventional analyses of preterm electroencephalography (EEG). **A**, Mean number of interburst intervals (IBIs) > 1 s (±SEM) for the three intraventricular hemorrhage (IVH) categories. No significant differences were found. **B**, Total burst counts (±SEM) demonstrating that short bursts (*dark blue bar*, 200 ms–2 s) and longer duration bursts (*light blue bar*, 2–6 s) in the three categories did not exhibit significant group differences. **C**, Example of EEG epoch (*black*) from infant with no IVH, with corresponding amplitude envelope (*blue*). **D**, Overlay of all amplitude envelope signals (*gray*) and their mean (*black*) for a single infant with no IVH. **E**, Example of EEG epoch for infant with IVH grade 2. **F**, All amplitude envelopes for an infant with IVH grade 2.

mid-duration bursts (1–3.5 s) differed significantly between IVH infants versus no IVH infants (**Fig. 4*D***). The difference in longer bursts (> 2 s duration) was statistically significant between pre-US-IVH and US-IVH infants when contrasted with no IVH infants (pre-US-IVH: $F = 6.91$, $p = 0.014$; US-IVH: $F = 24.01$, $p = 5.23 \times 10^{-5}$) (**Fig. 4*E***), indicating that IVH infants tend to have more asymmetric bursts. No significant difference was seen in Σ values between IVH severity grades ($F = 0.41$; $p = 0.53$).

Diagnostic Accuracy of Burst Shape Metrics

The accuracy of burst shape metrics in identifying IVH was evaluated by use of ROC curves for mean sharpness (*K*) (**Fig. 4*C***) and symmetry (Σ) derived from longer bursts (> 2 s duration) (**Fig. 4*F***). We combined IVH 1–2 and IVH 3–4 (injury positive) in both pre-US-IVH and US-IVH groups and compared these infants with infants who did not develop IVH for each burst measure.

The overall accuracy estimated by AUC was high in both groups (0.83–0.94). Importantly, sensitivity was fairly high (> 80% and > 60% for *K* and Σ, respectively) at all cutoff levels. A modest increase in sensitivity comes at a high price of substantial loss in specificity. We then tested systematically a range of *K* and Σ values for long bursts (> 2 s duration) and found high sensitivity and specificity at selected cutoff levels for all pre-US-IVH and IVH groups. Specifically, for this dataset, in both pre-US-IVH and US-IVH groups, we find that for *K* very high sensitivity and specificity values are found at a cutoff of –0.99 (for *K* ranging between –1.06 and –0.98). Similarly, for Σ, sensitivity and specificity in pre-US-IVH and US-IVH groups also remain high at a cutoff of 0.13 (for Σ ranging between 0.12 and 0.16). The validity of our results is confirmed by reliability tests, where the leave-one-out and added data permutation analyses reveal that for both *K* and Σ values, sensitivity and specificity remain consistently high (> 80% for *K* and Σ). **Table 2** summarizes the highest sensitivity and specificity values found in the ROC analysis along with the reliability tests employed.

DISCUSSION

This study shows that two novel features of early cortical activity in extremely preterm infants—burst shape and asymmetry—are sensitive indicators of IVH. Cortical burst shapes can be rapidly and automatically analyzed from continuously recorded EEG data: the presently used metrics are thus readily translatable back into the clinical setting. Our study also shows that these same metrics provide high diagnostic accuracy for the identification of early IVH. Together, these findings hold promise for the everyday clinical challenge of real-time detection of

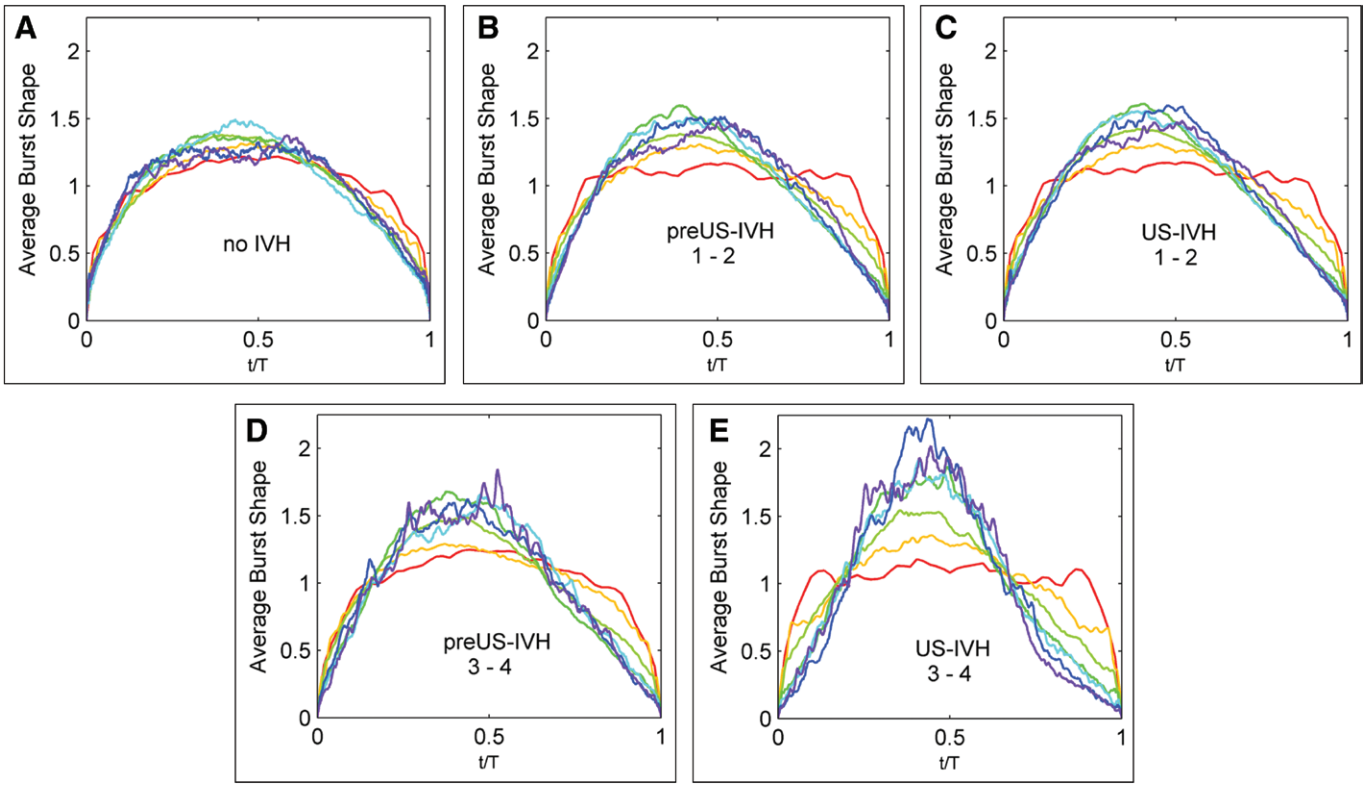

Figure 3. Differences in average burst shape across burst durations for infants with no intraventricular hemorrhage (IVH) compared with pre-ultrasound-confirmed (US-IVH) and US-IVH. Color coding of burst duration (200 ms–6 s) as per Figure 1. **A,** Grand average burst shape of all infants with no IVH: short and long bursts have similar symmetry and sharpness. **B,** Infants classified as mild-moderate exhibit changes in average burst shape pre-US-IVH over these burst durations hours before (**C**) presenting with grade 1 or 2 US-IVH. The onset of more severe hemorrhage is significantly noticeable in grand average shape features in infants pre-US-IVH (**D**) and in US-IVH (**E**) grades 3 or 4.

impending IVH in extremely preterm infants. Such a bedside method would also open a window to studying the pathophysiologic mechanisms leading to IVH that is required for developing novel, evidence-based therapeutic approaches.

Prior studies of EEG abnormalities in the presence of hemorrhagic lesions have focused on late EEG features, particularly the presence of PRS waves (26, 27). These PRS waves are identified as sharp, discrete transients of short duration (≤ 400 ms), which provide a relatively reliable sign of previously experienced IVH and white matter injury. The overall levels of early amplitude-integrated EEG (aEEG)/EEG activity were recently shown to be associated with early brain injury (10–12, 28, 29). Our objective and patient-wise adaptive analysis method found no significant quantitative differences between study groups in the conventional measures used in studies of aEEG markers during acute IVH, namely IBI and burst count. However, average shapes analysis of EEG reveals significantly sharper and more asymmetric bursts during the onset and occurrence of IVH as compared to infants without IVH. This suggests that the study of burst morphology in EEG may reflect disturbances in cortical activity prior to and during acute brain injury.

The observed changes in cortical burst shapes offer new insights into developmental neurobiology. Recent advances in experimental animal models have established that the early preterm EEG bursts are cortical events, SATs (30), that play a crucial role in both neuronal survival and guidance of emerging network growth (31, 32). Studies in both animals (32–34) and humans (35) have shown that these events bind brain areas together, a necessary activity-dependent developmental mechanism for the developing brain connectome (36, 37). It has also been demonstrated that the subplate layer in the developing cortex is responsible for orchestrating early cortical activity transients (38). These mechanisms offer a potential developmental context to our finding—burst shapes were found to be most informative in the most severe, parenchymal brain lesions that extend to subplate or its vicinity (i.e., IVH grades 3–4). A change in the shape of scalp EEG bursts to sharper and leftward asymmetric forms could arise from a compromised subplate function or from lesions in cortico-cortical tracts in the white matter, both of which may render cortical bursts more focal. Our recent theoretical work also suggests that changes in burst shapes may also arise from compromises in metabolic resources (20, 39)—that is, the availability of substrates essential to neuronal function, such as intracellular adenosine triphosphate and extracellular calcium. This is a likely scenario at or around the time of the occurrence of IVH.

Prospective trials are required to determine the utility of our approach prior to clinical implementation. Testing the proposed methodology in prospective cohorts would provide an indication of diagnostic efficacy during bedside monitoring. Prospective studies could be used to identify the critical

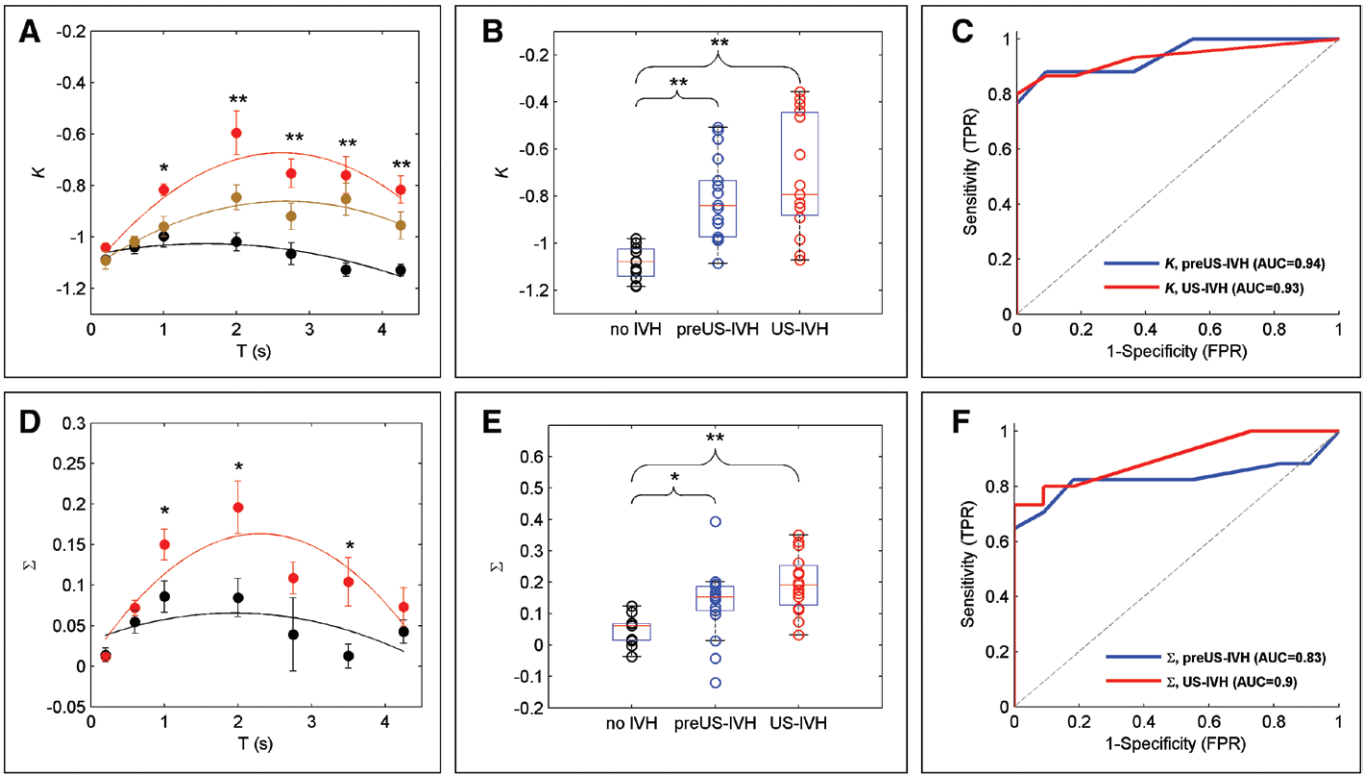

Figure 4. Summary of statistical differences in burst features between infants with no intraventricular hemorrhage (IVH) compared with those with any IVH grade (*$p < 0.05$; **$p < 0.01$). **A**, Infants with no IVH (*black*) had lower mean *K* values over longer bursts than infants with IVH 1–2 (*light brown*) and IVH 3–4 (*red*). **B**, Boxplots of no IVH (*black circles*) versus prior to ultrasound-confirmed IVH (pre-US-IVH) (*blue circles*) and ultrasound-confirmed IVH (US-IVH) (*red circles*) for mean values of $K > 2$ s, where *open colored circles* indicate individual data points. **C**, Receiver operating characteristic (ROC) curves showing true-positive rates (TPR) and false-positive rates (FPR) for mean *K* derived from bursts > 2 s in infants pre-US-IVH (blue) and US-IVH (*red*); the area under the curve (AUC) values suggest a high predictive value. **D**, Infants with no IVH (*black*) had lower mean Σ values over longer bursts compared with infants with IVH (*red*). Error bars denote ±SEM. *Solid curves* are parabolic fits. **E**, Boxplots of no IVH (*black circles*) versus pre-US-IVH (*blue circles*) and US-IVH (*red circles*) for mean values of Σ longer than 2 s, where *open colored circles* indicate individual data points. **F**, ROC curves for mean Σ for bursts > 2 s for all grades of pre-US-IVH (blue) and US-IVH (*red*) with the respective AUC values.

TABLE 2. Sensitivity and Specificity for Different Cutoffs in Mean Sharpness (*K*) and Mean Asymmetry (Σ) to Predict No Intraventricular Hemorrhage or Intraventricular Hemorrhage at Any Grade

Reliability Tests	pre-US-IVH (Sensitivity, Specificity)	US-IVH (Sensitivity, Specificity)
Receiver operating characteristic analysis	*K*: 88.2%, 91%	*K*: 86.7%, 90.9%
	Σ: 82.4%, 81.8%	Σ: 80%, 90.9%
Leave-one-out permutation	*K*: 83%, 90.3%	*K*: 88%, 90.3%
	Σ: 83%, 88.2%	Σ: 81%, 92.3%
Added data permutation	*K*: 80%, 91.9%	*K*: 88%, 91.9%
	Σ: 80%, 88.2%	Σ: 82%, 91.7%

US-IVH = ultrasound-confirmed intraventricular hemorrhage.
The top row shows the sensitivity and specificity of our main test statistics. The middle row shows the average sensitivity and specificity if leaving out any one of the subjects. The lower row shows the values if further infants without the reported effect are added.

time windows in which the present markers (e.g., increasing burst sharpness) signify the occurrence of IVH. The rapid and robust characterization of burst activity could thus be used to trigger a cranial ultrasound and relevant treatment protocol. Furthermore, such studies would clarify whether these EEG metrics reveal as-yet-unmeasured existing IVH or are sensitive to precursors that predict the onset of IVH itself. For example, this could be achieved using frequent, repeated ultrasounds. Importantly, the robustness to relatively short epochs of data (< 90 min), rather than hours of continuously recorded EEG (which are then subjected to laborious visual assessment), would facilitate efficient prospective study design. Such larger

studies would also have the power to detect relatively common chronic sequelae of IVH such as periventricular leukomalacia.

Prior to routine clinical implementation, our methodology requires validation from larger, independent patient cohorts that are monitored with EEG for several days after birth, with detailed accounts of clinical treatment, complications, outcome, and other comorbidities. A larger cohort size necessitates a multicenter study or, optimally, sourcing existing datasets with similar data quality, clinical details, and outcome-related information. For future application, testing this study's methodology in prospective cohorts would provide an indication of diagnostic efficacy during bedside monitoring.

Our present method helps alleviate common challenges in continuous brain monitoring during neonatal intensive care. Specifically, our method analyzes extracted EEG events (bursts) without a need for continuous, uninterrupted streams of EEG signal. This allows automated selection of sufficient quality, artifact-free EEG epochs, without compromising analytical reliability. Hence, our burst-shape metrics will allow reliable diagnostics derived from EEG monitoring, even during NICU treatment where EEG records are frequently prone to disruption by clinical care artifacts, which are a particular weakness of currently available algorithms for NICU EEG monitoring.

In conclusion, we demonstrate that burst shape and burst asymmetry in the early EEG are indicators of IVH in extremely preterm infants as soon as 12 hours after birth. Early and accurate identification of abnormal burst shape and asymmetry may enable timely identification of infants at high risk for developing IVH and may thus contribute to an increased understanding of pathophysiologic mechanisms associated with IVH and targeted neuroprotective strategies.

REFERENCES

1. Ballabh P: Intraventricular hemorrhage in premature infants: Mechanism of disease. *Pediatr Res* 2010; 67:1–8
2. Bolisetty S, Dhawan A, Abdel-Latif M, et al; New South Wales and Australian Capital Territory Neonatal Intensive Care Units' Data Collection: Intraventricular hemorrhage and neurodevelopmental outcomes in extreme preterm infants. *Pediatrics* 2014; 133:55–62
3. Milligan DW: Failure of autoregulation and intraventricular haemorrhage in preterm infants. *Lancet* 1980; 1:896–898
4. Volpe JJ: Neurobiology of periventricular leukomalacia in the premature infant. *Pediatr Res* 2001; 50:553–562
5. Volpe JJ: Brain injury in premature infants: A complex amalgam of destructive and developmental disturbances. *Lancet Neurol* 2009; 8:110–124
6. McCrea HJ, Ment LR: The diagnosis, management, and postnatal prevention of intraventricular hemorrhage in the preterm neonate. *Clin Perinatol* 2008; 35:777–792, vii
7. Ballabh P: Pathogenesis and prevention of intraventricular hemorrhage. *Clin Perinatol* 2014; 41:47–67
8. Bada HS, Hajjar W, Chua C, et al: Noninvasive diagnosis of neonatal asphyxia and intraventricular hemorrhage by Doppler ultrasound. *J Pediatr* 1979; 95:775–779
9. Hayakawa F, Okumura A, Kato T, et al: Determination of timing of brain injury in preterm infants with periventricular leukomalacia with serial neonatal electroencephalography. *Pediatrics* 1999; 104:1077–1081
10. Okumura A, Hayakawa F, Kato T, et al: Developmental outcome and types of chronic-stage EEG abnormalities in preterm infants. *Dev Med Child Neurol* 2002; 44:729–734
11. Olischar M, Klebermass K, Waldhoer T, et al: Background patterns and sleep-wake cycles on amplitude-integrated electroencephalography in preterms younger than 30 weeks gestational age with peri-/intraventricular haemorrhage. *Acta Paediatr* 2007; 96:1743–1750
12. Chalak LF, Sikes NC, Mason MJ, et al: Low-voltage aEEG as predictor of intracranial hemorrhage in preterm infants. *Pediatr Neurol* 2011; 44:364–369
13. Watanabe K, Hayakawa F, Okumura A: Neonatal EEG: A powerful tool in the assessment of brain damage in preterm infants. *Brain Dev* 1999; 21:361–372
14. Olischar M, Klebermass K, Kuhle S, et al: Reference values for amplitude-integrated electroencephalographic activity in preterm infants younger than 30 weeks' gestational age. *Pediatrics* 2004; 113:e61–e66
15. Wikström S, Pupp IH, Rosén I, et al: Early single-channel aEEG/EEG predicts outcome in very preterm infants. *Acta Paediatr* 2012; 101:719–726
16. Vanhatalo S, Kaila K: Development of neonatal EEG activity: From phenomenology to physiology. *Semin Fetal Neonatal Med* 2006; 11:471–478
17. André M, Lamblin MD, d'Allest AM, et al: Electroencephalography in premature and full-term infants. Developmental features and glossary. *Neurophysiol Clin* 2010; 40:59–124
18. Vanhatalo S, Kaila K: Spontaneous and evoked activity in the early human brain. *In:* The Newborn Brain: Neuroscience & Clinical Applications. Lagercrantz H (Ed). Cambridge: Cambridge University Press, 2009, pp 229–243
19. Aso K, Abdab-Barmada M, Scher MS: EEG and the neuropathology in premature neonates with intraventricular hemorrhage. *J Clin Neurophysiol* 1993; 10:304–313
20. Roberts JA, Iyer KK, Finnigan S, et al: Scale-free bursting in human cortex following hypoxia at birth. *J Neurosci* 2014; 34:6557–6572
21. Iyer KK, Roberts JA, Metsäranta M, et al: Novel features of early burst suppression predict outcome after birth asphyxia. *Ann Clin Transl Neurol* 2014; 1:209–214
22. Hayakawa M, Okumura A, Hayakawa F, et al: Background electroencephalographic (EEG) activities of very preterm infants born at less than 27 weeks gestation: A study on the degree of continuity. *Arch Dis Child Fetal Neonatal Ed* 2001; 84:F163–F167
23. Wikström S, Lundin F, Ley D, et al: Carbon dioxide and glucose affect electrocortical background in extremely preterm infants. *Pediatrics* 2011; 127:e1028–e1034
24. Papile LA, Burstein J, Burstein R, et al: Incidence and evolution of subependymal and intraventricular hemorrhage: A study of infants with birth weights less than 1,500 gm. *J Pediatr* 1978; 92:529–534
25. de Vries LS, Eken P, Dubowitz LM: The spectrum of leukomalacia using cranial ultrasound. *Behav Brain Res* 1992; 49:1–6
26. Clancy RR, Tharp BR, Enzman D: EEG in premature infants with intraventricular hemorrhage. *Neurology* 1984; 34:583–590
27. Okumura A, Hayakawa F, Kato T, et al: Positive rolandic sharp waves in preterm infants with periventricular leukomalacia: Their relation to background electroencephalographic abnormalities. *Neuropediatrics* 1999; 30:278–282
28. Hellström-Westas L, Klette H, Thorngren-Jerneck K, et al: Early prediction of outcome with aEEG in preterm infants with large intraventricular hemorrhages. *Neuropediatrics* 2001; 32:319–324
29. Bowen JR, Paradisis M, Shah D: Decreased aEEG continuity and baseline variability in the first 48 hours of life associated with poor short-term outcome in neonates born before 29 weeks gestation. *Pediatr Res* 2010; 67:538–544
30. Vanhatalo S, Palva JM, Andersson S, et al: Slow endogenous activity transients and developmental expression of K+-Cl- cotransporter 2 in the immature human cortex. *Eur J Neurosci* 2005; 22:2799–2804
31. Hanganu-Opatz IL: Between molecules and experience: Role of early patterns of coordinated activity for the development of cortical maps and sensory abilities. *Brain Res Rev* 2010; 64:160–176
32. Colonnese M, Khazipov R: Spontaneous activity in developing sensory circuits: Implications for resting state fMRI. *Neuroimage* 2012; 62:2212–2221
33. Kilb W, Kirischuk S, Luhmann HJ: Electrical activity patterns and the functional maturation of the neocortex. *Eur J Neurosci* 2011; 34:1677–1686

34. Brockmann MD, Pöschel B, Cichon N, et al: Coupled oscillations mediate directed interactions between prefrontal cortex and hippocampus of the neonatal rat. *Neuron* 2011; 71:332–347
35. Omidvarnia A, Fransson P, Metsäranta M, et al: Functional bimodality in the brain networks of preterm and term human newborns. *Cereb Cortex* 2014; 24:2657–2668
36. Zhang LI, Poo MM: Electrical activity and development of neural circuits. *Nat Neurosci* 2001; 4(Suppl):1207–1214
37. Rubinov M, Sporns O, van Leeuwen C, et al: Symbiotic relationship between brain structure and dynamics. *BMC Neurosci* 2009; 10:55
38. Dupont E, Hanganu IL, Kilb W, et al: Rapid developmental switch in the mechanisms driving early cortical columnar networks. *Nature* 2006; 439:79–83
39. Roberts JA, Iyer KK, Vanhatalo S, et al: Critical role for resource constraints in neural models. *Front Syst Neurosci* 2014; 8:154